Journal of Chemical Ecology, Vol. 31, No. 1, January 2005 (© 2005)

DIVERGENCE OF STREAMLINES APPROACHING A PECTINATE INSECT ANTENNA: CONSEQUENCES FOR CHEMORECEPTION

CATHERINE LOUDON* and ELIZABETH C. DAVIS

Department of Ecology and Evolutionary Biology
University of Kansas, Lawrence, Kansas 66045-7534, USA

(Received April 14, 2004; accepted August 10, 2004)

Abstract—Pectinate (feathery) antennae have high resistance to air flow, and therefore most of the air approaching an antenna is diverted around it and is not available for chemical sampling by the sensory hairs on that antenna. The small fraction (approximately 10–20%) of approaching air that passes through the air spaces or gaps in the antenna decelerates and the streamlines diverge as the air approaches the antenna. Sampling a small fraction of air that is decelerating and diverging has consequences for chemoreception that are described here for the first time. The behavior of the air is predicted from application of a fluid mechanical law: the principle of continuity. As this small fraction of air decelerates and flows through the air gaps in the antenna, it will be "stretched" in the plane perpendicular to the air flow. Therefore, the air may be sampled by the sensory hairs at a greater spatial resolution than expected from the distribution of the odorant molecules in the air upstream of the antenna. However, the slowing down of odorant-laden air as it passes through an antenna will not change the perceived temporal characteristics of the chemical stimulus (e.g., the rate of odorant filament encounter). This distortion or stretching of the air sample is expected to develop within about one antennal width upstream of the antenna, as verified by examining wakes of simple physical models.

Key Words—Antenna, insect, flow, chemoreception, pheromone, pheromone plume, spatial heterogeneity.

INTRODUCTION

The pectinate insect antennae have thousands to tens of thousands of sensory hairs arrayed in complex arrangements in three-dimensional space (e.g., Steinbrecht, 1970). Whereas such a large number of chemosensory hairs should facilitate the

* To whom correspondence should be addressed. E-mail: loudon@ku.edu

capture of odorant molecules from the air, Vogel (1983) noted that such a dense array of hairs would have a high resistance to air movement and, therefore, decrease the amount of air sampled by those hairs. This has been verified for the pectinate antennae of two insect species: only 10–20% of the approaching air passed through the pectinate antennae of the luna moth, *Actias luna* (L.) (Vogel, 1983) and the silkworm moth, *Bombyx mori* (L.) (Zhang, 2001; Zhang and Loudon, unpublished). A "trade-off" exists between the amount of air processed and the efficiency with which that air is sampled by the sensory hairs. For pectinate antennae, this small fraction of air is sampled with great efficiency (Loudon and Koehl, 2000). There will be additional consequences of this particular air flow pattern that have not been considered in the literature until now.

Some general features of this diverging and decelerating air flow pattern may be predicted by applying the fluid mechanical "principle of continuity." The principle requires that air approaching a pectinate antenna will decelerate and, thus, its streamlines will diverge (splay downstream). For air containing a spatially-heterogeneous odorant, divergence will distort the plume, affecting its interception by chemosensory structures. Odorants have a patchy distribution in natural environments, with filaments of concentrated odorant interspersed with clean air (Murlis and Jones, 1981; Murlis, 1986; Murlis et al., 1990). The filamentous nature of odorants is used during orientation to odor sources by some insect species (Vickers and Baker, 1994; Willis et al., 1994; Fadamiro and Baker, 1997; Baker et al., 1998; Vickers et al., 2001).

The principle of continuity is a statement of the conservation of mass applied to a moving fluid such as air or water. If only 10–20% of the air approaching a pectinate antenna passes through, then the approaching air must diverge (the streamlines will splay) (Figure 1A and B). By definition, a streamline is tangent to the local flow at every point, which means that a streamline will not be crossed even though it is not a solid barrier. Therefore, conservation laws may be applied to a volume enclosed within a set of streamlines (a "streamtube"), and the mass of air entering this volume must be identical to the mass of air leaving this volume during the same time period (if air moleculer are not created, destroyed, or accumulated within this volume). Air volume may be substituted for mass, assuming air of constant density (valid under these subsonic, biologically-relevant conditions). It follows that the product of cross-sectional area and average velocity will be constant at every downstream location (Figure 1A). Therefore, as the cross-sectional area increases (as the streamlines diverge), the average velocity will decrease. If the flow pattern is not changing over time, a streamline will indicate the path that will be traced by an individual fluid particle as it moves downstream in the flow (see Vogel 1994, for more explanation). Any patches or filaments of odorant will be distorted in space as each patch follows its own set of streamlines, slowing and diverging. The principle of continuity predicts that patches of odorant in air approaching a pectinate antenna will be stretched in the plane perpendicular to

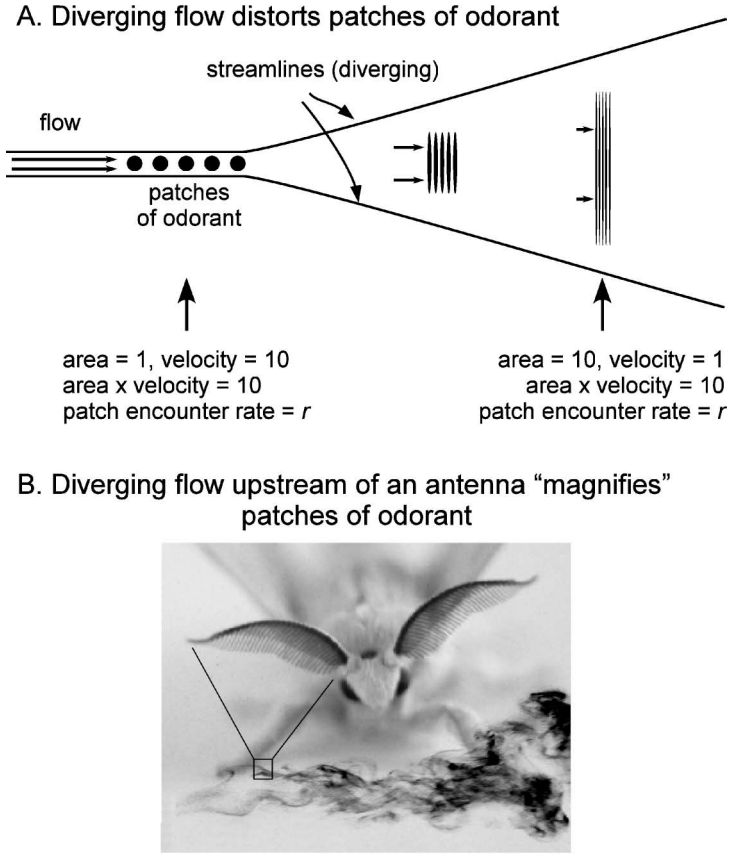

FIG. 1. (A) Patches of odorant, shown at left as black circles, become distorted in shape as the streamlines of the air diverge and the flow slows. Arrows indicate the direction of the air flow, with speed represented by arrow length. The representative values for area, velocity, and patch encounter rate demonstrate the predictions from the principle of continuity: the constant product of area × velocity (between streamlines) and the unchanging patch encounter rate. (B) The picture of the moth shows how an odorant plume will be magnified (stretched) as it is sampled by a pectinate antenna.

the direction of air flow and shortened in the direction of air flow (Figure 1A). A stretched, thinner patch of odorant will have the opportunity to strike a larger number of sensory hairs, but the patch encounter rate by an individual sensory hair is not expected to change. This is because the odorant patches are thinned and slowed by the same factor as they approach an antenna (Figure 1A).

Although the principle of continuity predicts that the air approaching a pectinate antenna will decelerate and diverge, it does not predict how far upstream of

the antenna this divergence will occur. The farther upstream the divergence occurs, the greater the opportunity for the thinner, stretched filaments (Figure 1A) to be eroded by diffusion and the less likely to be detected by the antennae as discreet filaments. It is not known where streamlines start to diverge upstream of a porous bluff body ("bluff" means nonstreamlined), such as a pectinate antenna.

In general, the location of the divergence upstream of a body will depend on the geometry and the magnitude of the Reynolds number (a dimensionless number characterizing the ratio of inertial to viscous effects in a fluid). The Reynolds number is defined as $Re = \rho L v/\mu$, where ρ is the density of the fluid, L is the characteristic length, v is the velocity, and μ is the kinematic viscosity of the fluid. The characteristic length of the object is usually measured perpendicular to the direction of flow, and the velocity of the fluid is measured with respect to the object's frame of reference (Vogel, 1994). Most of the literature on porous structures is for higher Reynolds number cases (Elder, 1959; Lau and Baines, 1968; Castro, 1971; Koo and James, 1973; Castro, 1976) in which the upstream divergence is extremely close to the body. For lower Reynolds numbers (relevant to insect antennae), diverging flow could develop farther upstream because of the increased importance of viscous effects.

To estimate where the flow diverges around porous structures for lower Reynolds numbers, we measured the flow around physical models of arrays of platinum wires. Because of the technical difficulties with accurate measurements of upstream streamlines, we measured downstream flow because it allowed us to identify unambiguously the fluid parcel that had moved through the porous array. These downstream measurements may be used to predict upstream streamlines because upstream and downstream flow patterns will be symmetrical for low Reynolds number flow ($Re < 1$). The downstream convergence will start to extend farther from the body than the upstream divergence as the Reynolds number increases above one (White, 1991). Therefore, measurements for this higher Reynolds number range ($Re > 1$) based on the downstream convergence will be a conservative estimate (in this case, overestimate) of the extent of the upstream divergence.

Dimensionless modeling was used (matching the Reynolds number of the physical model with the relevant Reynolds number for antennae) to enable comparison of the flow around the model array with air flow around insect antennae. A shift from air to water at the same Reynolds number range will not change the flow pattern geometry, which is the logic behind dimensionless modeling. The implications of the principle of continuity as described here are relevant for chemoreception in air or water.

METHODS AND MATERIALS

Physical Models and Flow Chamber. The physical model consisted of an array of platinum wires inside a fluid-filled enclosed chamber (with a glass top

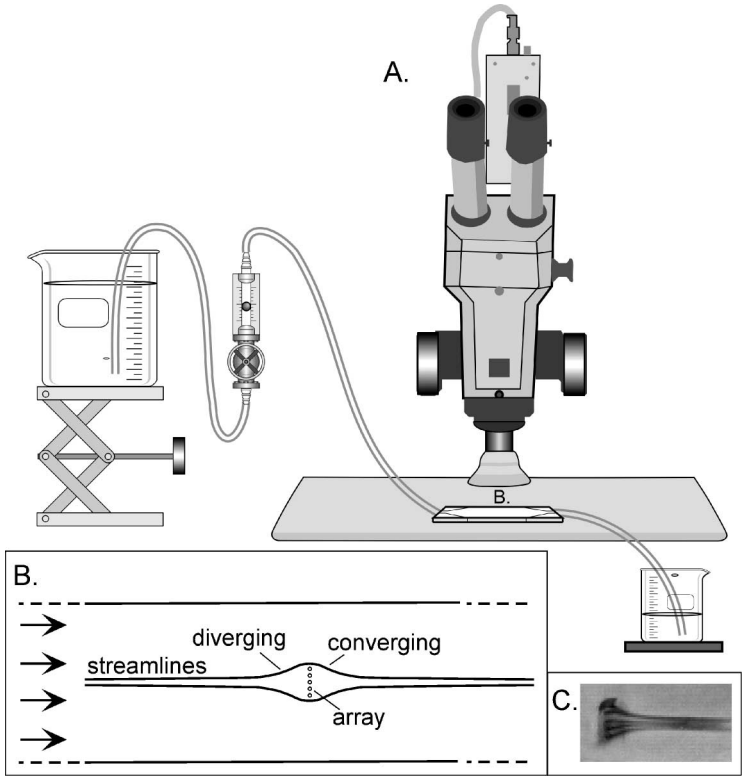

FIG. 2. Flow visualization technique: A—Experimental setup showing location of visualization chamber on microscope. B—Camera/microscope view of chamber showing array (5 parallel wires viewed end-on) and two hypothetical streamlines diverging upstream of the array (with symmetrical downstream convergence). C—Frame from videotape showing streaklines of marked thymol blue solution downstream of the array.

for viewing) (Figure 2). The array had five parallel wires (wire diam = 0.3 mm, length 3.0 mm, array width 4.28 mm). The platinum wires of the physical model were used as the anodes to mark the fluid at the array itself; a single platinum wire elsewhere in the chamber served as the cathode. The applied voltage was 1.7 V. This array was centered in a chamber of 3.0-mm height and 28-mm width (Figure 2A). Therefore, the wires completely spanned the height of the chamber to make the flow two-dimensional, and the array spanned 20% of the total cross-sectional area of the chamber. To generate higher resistance to flow (lower porosity) as a second treatment, a nylon mesh sheath was placed over the array of wires.

Gravity-driven flow of the solution through the chamber was controlled and measured by a flow meter (Manostat flow meter #2, New York). For each array

type, three different volumetric flow rates were tested, each corresponding to a different Reynolds number. For these Reynolds numbers, the flow was laminar (not turbulent). Three Reynolds numbers were used for each array type: 0.5, 1, and 3 (using chamber height, 3 mm, as characteristic length L). The volumetric flow rates were kept within 5% of the target flow rate. The complete range of fluid speeds inside the chamber ranged from 0.02 cm/sec to 0.138 cm/sec. The range of fluid temperatures was 19–23°C.

Physical Properties of Fluid Used for Flow Visualization

An aqueous solution of the pH indicator thymol blue (0.05 g thymol blue and 1.52 g NaCl in 500 ml water) was used to visualize the flow. This fluid can be "marked" electrolytically when titrated just below the pH at which it changes color from amber to blue (pH 8, Baker, 1966; Sparrow et al., 1970). We added salt (NaCl) to the original published recipe (only thymol blue in water) in order to increase the electrical conductivity of the solution and decrease the amount of hydrogen bubbles generated. The fluid was marked at the array of wires and the resulting streaklines in the chamber were videotaped (Panasonic WV-CL700 camera mounted on a Nikon Stemi SV6 dissecting microscope). The advantage of this flow visualization technique is that the marked fluid does not differ in physical properties from the unmarked fluid, and therefore will accurately represent its behavior. The marked fluid eventually reverts back to its original unmarked state; this change was imperceptible over the time period of our measurements. We tested this by repeatedly digitizing marked patches of fluid as the fluid moved downstream. The digitized areas did not change over the videotaping period (up to a minute). This was tested for three replicates for each of three different flow rates. The area of the marked fluid was not significantly affected by flow speed (ANCOVA, $P = 0.87$, $N = 9$) or distance downstream ($P = 0.98$).

The physical properties of the solution were determined within the range of fluid temperatures used in the experiments (19–23°C). The density of the solution was determined by weighing three 100 ml samples (in a 100 ml volumetric flask) at 20°C. The average density of the solution was 0.99923 ± 0.00056 g/ml (mean $\pm$ 1 SD, $N = 3$), 0.09% greater than pure water at that same temperature (0.99823 g/ml, Weast et al., 1988). Therefore, the density of pure water was used for the density of the thymol blue solution in all subsequent calculations. The viscosity of the solution was measured for three replicates at each of two temperatures (20°C and 25°C) using a Gilmont falling ball viscosimeter (Barnant Company, Barrington, IL) and it was always within 2% of the value reported for pure water (Weast et al., 1988). Comparable measurements performed on deionized water were of similar accuracy (within 3% of the published value for pure water). Therefore, the viscosity of pure water was used for the viscosity of the thymol blue solution in all subsequent calculations.

Video Analysis

Regular speed video (30 frames/sec) was digitized using motion analysis software (Motus, Peak Performance Inc., Englewood, CO). The distance between the two outermost streamlines ("width of marked fluid") was digitized at multiple locations (up to 18 locations; 3 replicates for each *Re* and resistance) downstream of the array at 1.2 or 0.25 mm intervals (the finer spatial scale was used for the less porous/higher resistance array). From these digitized points, we were able to calculate the change in width of the marked fluid as it moved farther downstream from the array. These widths were normalized to a 0–1 scale where "1" is the width of the marked fluid at the array for each porosity. When we were no longer able to measure further change in the width (successive widths differed by a pixel or less and no longer showed a monotonic trend), we considered the streamlines to have "converged" to a constant distance apart.

Statistical Analysis and Mathematical Manipulations

All statistics were performed with SAS software (version 8.2, SAS Institute Inc., Cary, NC). Exponential fits to the widths of the marked fluid (Figure 3) were calculated by using Excel's built-in exponential regression option after subtracting the constant asymptotic value (for large x). Streamlines around a sphere at low

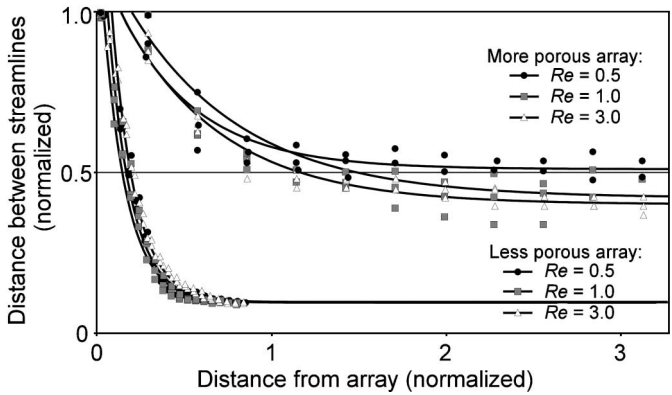

FIG. 3. Streamlines of the fluid that had passed through the array converged more rapidly downstream for the less porous array (with higher resistance to flow). The porosity (the normalized distance between streamlines far downstream of the array) did not differ within the Reynolds number range (0.5–3.0) for the less porous array, but decreased slightly with Reynolds number for the more porous array. Each symbol represents a single replicate, and the lines indicate best exponential fits to the data for each Reynolds number and array type. The distance between streamlines was normalized to the width of the marked fluid at the array, whereas the distance downstream was normalized to array width.

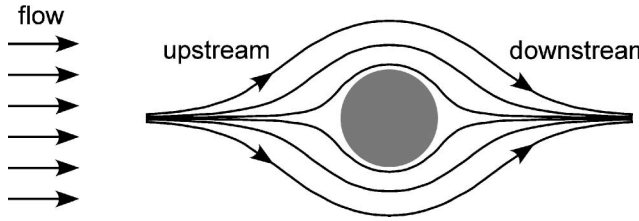

FIG. 4. Streamlines around a sphere at low Reynolds number (calculated from Stokes' equations) show the upstream/downstream symmetry expected for small bodies or in slow flow.

Reynolds number were calculated from Stokes' equations of the velocity flow field (Equation 3-214 in White, 1991) by a stepwise iterative simulation calculating the next position of a fluid particle from its current position and velocity vector (Figure 4).

RESULTS

Physical Modeling

The marked fluid downstream of the five-membered array (Figure 2C) was used to identify the locations of the streamlines of the fluid that had passed through the array (marked at the array elements). The distance between the two outermost streamlines decreased downstream of the array asymptotically to an approximately constant value (Figure 3). This value was compared to the distance between the same streamlines at the array. The streamline width ratio (width far downstream: width at array) was used to estimate the porosity of the array (the amount of approaching fluid that passes through the array). The average porosity of the high resistance array was $9.7 \pm 0.08\%$ (mean $\pm$ 1 SD, $N = 3$ *Re*) and the average porosity of the low resistance array was $44 \pm 6\%$ (mean $\pm$ 1 SD, $N = 3$ *Re*). The porosities were significantly different for the two different array resistances; the porosity of the low resistance array decreased slightly with increasing Reynolds number, whereas the porosity of the high resistance array was independent of Reynolds number for the range of parameters and resistances used (two-way ANOVA, $P < 0.001$ for array resistance, $P = 0.04$ for Reynolds number, $P = 0.04$ for the *Re* $\times$ resistance interaction term; $N = 3$ replicates for each of 3 Reynolds numbers for each resistance level).

Convergence took place within one array diameter downstream for the less porous array (entire *Re* range 0.5–3) and within two array diameters for the more porous array (entire *Re* range 0.5–3). That is, the distance between the outermost streamlines did not continue to decrease farther downstream.

DISCUSSION

It is not intuitive that a parcel of air approaching a pectinate antenna will be "stretched" in the plane perpendicular to flow, although this streamline divergence is mandated by the fluid mechanical principle of continuity. This divergence of the flow has important consequences for chemoreception by pectinate antennae because it will affect the spatial pattern with which the odorant molecules encounter the sensory hairs on an antenna. For pectinate antennae, the parcel of air will be stretched by a factor of $5x$–$10x$ because these antennae typically sample only about 10–20% of the approaching air. For example, a patch of odorant that is 1 mm^2 across (upstream) could be enlarged to 5–10 mm^2 across when it arrives at the sensory hairs. From the perspective of the sensory hairs, it appears as if the patch is magnified; i.e., a larger number of sensory hairs will encounter a patch of odorant than would be expected from the size of the patch upstream. Whether this stretching is two-dimensional (within the plane perpendicular to flow) vs. one-dimensional (along a single axis within that plane), is not known and could differ for antennae of different morphology. Note that simply changing the shape of an odorant patch (and not its volume) will not change the odorant concentration in that patch. The patch volume remains constant because as the patch is stretched in the plane perpendicular to flow, it will be shortened in the direction parallel to flow (Figure 1).

Over time, diffusion will reduce the differences in concentration between the odorant patches and the intervening clean air, making that air sample more homogeneous. The elongation and thinning of the patches that occurs during streamline divergence (e.g., Figure 1) will greatly increase the surface area of the patches and, therefore, the rate of homogenization of the air. If the streamline divergence is far upstream of an antenna, there will be more time for this diffusion-driven homogenization to occur, and the potential information in the filamentous odorant pattern could be lost or diminished far more rapidly. In addition, this homogenization may lower the concentration to a level below the detection threshold of the sensory array. To obtain an accurate picture of the extent to which a patchy or filamentous odorant pattern may linger or be obliterated, it is important to determine how far upstream of an antenna the streamline divergence will take place. The principle of continuity does not specify the location of streamline divergence, but only that it will occur.

It is reasonable, as a first approximation, to assume that flow around a slightly porous structure (such as a pectinate insect antenna) might resemble flow around a solid object with the same outer dimensions. The velocity flow field around a solid sphere at low Reynolds number is a classic solution in fluid mechanics (Stokes' equations, Equation 3-214 in White, 1991; see streamlines calculated from these equations in Figure 4). However, flow through or around porous structures may sometimes exhibit complex or unexpected behavior, such as the pulsatile flow

generated by vortex shedding of a cylindrical array for certain combinations of geometry and flow conditions (Leonard, 1992), or the "pathological behavior" of the mathematical solutions for low Reynolds number flow through porous pipes (referring to lack of solutions, or multiple sets of double solutions, p. 148, White, 1991). In low Reynolds number flow, objects may have surprisingly large velocity boundary layers or may "feel" other objects or walls from very far away (Happel and Brenner, 1965; Loudon et al., 1994). The lack of published detail on streamline divergence upstream of porous objects in low Reynolds number flow supplied the motivation for making direct estimates of streamlines using physical modeling.

Theoretically, the distance between diverging (or converging) streamlines around an isolated body in an unbounded medium (Figure 4) will continue to approach a limit indefinitely, making it impossible to define a location at which divergence starts. In practice, however, it is useful to consider when most (90%) of the divergence (or convergence) has occurred. This definition is similar to the recommendation made by Vogel (1994, 2003) to use 90% of free stream velocity for identifying the depth of the velocity boundary layer (rather than the 99% definition used by fluid mechanical engineers). For example, streamlines passing closely around a solid sphere at low *Re* ($Re < 1$, streamlines passing within 5% of the sphere's diameter), will have converged 90% within one radius downstream of the sphere's surface (Figure 4, innermost streamlines).

Results from the physical modeling make it clear that most of the divergence of the air is likely to take place immediately upstream of a pectinate antenna for biologically relevant antennal morphologies and air flows. Therefore, there will be little chance for the increased homogenization of filaments and clean air caused by far-upstream diverging flow and distorted odorant patches. A pectinate antenna has porosity more similar to the "less porous" array used for these measurements, and, therefore, the divergence of the air is expected within about one array diameter upstream.

The experimental Reynolds number range (0.5–3) corresponds to cases of extremely slow flow or very small antennae, such as 1-mm wide antennae in air flows of a few cm/sec (calculated from the formula for *Re* given above, using $\rho/\mu = 15 \times 10^{-6}$ m^2/sec). For larger Reynolds number flow (larger antennae or faster air flow), the upstream divergence is expected to be even closer to the antenna (within one antennal width). No evidence was seen for complex or unexpected flow behavior; the streamlines converged smoothly downstream in a manner similar to streamlines downstream from a solid sphere in low Reynolds number flow (compare Figures 3 and 4).

Some pectinate antennae are flat (planar) and are held perpendicular to the oncoming air, similar to our experimental array (e.g., luna moth antennae, *A. luna*), whereas others are curved or bent in a "V" shape, such as antennae from gypsy moths [*Lymantria dispar* (L.)] and silkworm moths (*B. mori*), and are held with the

concave "V" oriented approximately upstream. While details of the streamlines passing through these antennae remain unexplored, experiments with curved or tilted screens placed in a flow field show that the streamlines approaching a screen surface tend to bend such that the flow always passes perpendicularly through the screen (Elder, 1959; Lau and Baines, 1968; Koo and James, 1973). In an analogous manner, the streamlines flowing through a curved or bent pectinate antenna are likely to deflect and pass through the mesh-like structure at right angles.

A physical model will capture the essential flow behavior at the antennal level if its Reynolds number (based on the whole antenna) and porosity are matched by the model, and if its geometry is similar. Therefore, the divergence pattern reported here will be most closely approximated by the flow approaching flat pectinate antennae, and will be similar to the flow approaching curved or "V" shaped pectinate antennae. Whereas the flow through an antenna could be affected by the presence of nearby surfaces including the head of the insect, we do not expect the streamlines to diverge in a qualitatively different manner from that described here. Flow through an antenna positioned into the flow is less likely to be affected by the proximity of the head.

The results presented in this paper are of interest when the odorants in the environment are of a patchy distribution and where the patches are much smaller than the antennae. If the odorant concentration is uniform everywhere (which is approximately true when the patch size greatly exceeds the size of the antenna), any divergence or mixing (within the patch) will have no effect on the odorant concentration at the sensory hairs. Sensory hairs on pectinate antennae are individually innervated (Steinbrecht, 1987, 1999) but are so small and close to each other that spatial heterogeneity in the odorant concentration at their spatial scale will only be meaningful in fast air flows, such as those generated during flying; i.e., for slow air speeds, the "random walks" taken by individual odorant molecules passing between sensory hairs exceed the distance between adjacent hairs (Loudon and Koehl, 2000). There is behavioral evidence for the importance of small scale sampling (within an antenna) by species with filamentous antennae (Liu and Haynes, 1992; Baker et al., 1998) although this is not yet demonstrated for an insect with pectinate antennae. How filamentous antennae stretch or distort an odorant pattern is not known, but the work of Schneider et al. (1998) with the sexually dimorphic antennae from *Manduca sexta* (L.) suggests that this small difference in antennal morphology will change the way in which chemicals are sampled. It is clear that pectinate antennae sample a "magnified" piece of the olfactory landscape, without much homogenization of this magnified patch. The prediction that the temporal pattern of filament interception will remain unchanged has recently been tested and verified by electroantennography on *B. mori* and *L. dispar* antennae (Bau, et al., in review).

Acknowledgments—This research was funded by a grant from the National Science Foundation to CL (IBN 9984475). We thank Bill McGregor and the Physics Shop for construction of the flow chamber with the platinum wire array. J. Botz, G. Miller, and two anonymous reviewers made constructive suggestions on the manuscript.

REFERENCES

BAKER, D. J. 1966. A technique for the precise measurement of small fluid velocities. *J. Fluid Mech.* 26:573–575.

BAKER, T. C., FADAMIRO, H. Y., and COSSÉ, A. A. 1998. Moth uses fine tuning for odor resolution. *Nature* 393:530.

CASTRO, I. P. 1971. Wake characteristics of two-dimensional perforated plates normal to an air-stream. *J. Fluid Mech.* 46:599–609.

CASTRO, I. P. 1976. Some problems concerning the production of a linear shear flow using curved wire-gauze screens. *J. Fluid Mech.* 76:689–709.

ELDER, J. W. 1959. Steady flow through non-uniform gauzes of arbitrary shape. *J. Fluid Mech.* 5:355–368.

FADAMIRO, H. Y. and BAKER, T. C. 1997. *Helicoverpa zea* males (Lepidoptera: Noctuidae) respond to the intermittent fine structure of their sex pheromone plume and an antagonist in a flight tunnel. *Physiol. Entomol.* 22:316–324.

HAPPEL, J. and BRENNER, H. 1965. Low Reynolds Number Hydrodynamics. Prentice Hall, Englewood Cliffs, NJ.

KOO, J. K. and JAMES, D. F. 1973. Fluid flow around and through a screen. *J. Fluid Mech.* 60:513–538.

LAU, Y. L. and BAINES, W. D. 1968. Flow of stratified fluid through curved screens. *J. Fluid Mech.* 33:721–738.

LEONARD, A. B. P. 1992. The biomechanics, autecology and behavior of suspension-feeding in crinoid echinoderms. PhD Dissertation. University of California, San Diego.

LIU, Y. B. and HAYNES, K. F. 1992. Filamentous nature of pheromone plumes protects integrity of signal from background chemical noise in cabbage looper moth, *Trichoplusia ni*. *J. Chem. Ecol.* 18:299–307.

LOUDON, C., BEST, B. A., and KOEHL, M. A. R. 1994. When does motion relative to neighboring surfaces alter the flow through arrays of hairs? *J. Exp. Biol.* 193:233–254.

LOUDON, C. and KOEHL, M. A. R. 2000. Sniffing by a silkworm moth: Wing fanning enhances air penetration through and pheromone interception by antennae. *J. Exp. Biol.* 203:2977–2990.

MURLIS, J. 1986. The structure of odor plumes, pp. 27–38, *in* T. L. Payne, M. C. Birch, and C. E. J. Kennedy (eds.). Mechanisms in Insect Olfaction. Clarendon Press, Oxford.

MURLIS, J. and JONES, C. D. 1981. Fine-scale structure of odor plumes in relation to insect orientation to distant pheromone and other attractant sources. *Physiol. Entomol.* 6:71–86.

MURLIS, J., WILLIS, M. A., and CARDÉ, R. T. 1990. Odour signals: Patterns in time and space, pp. 6–17, *in* K. Doving (ed.). Proceedings of the X International Symposium on Olfaction and Taste, Oslo.

SCHNEIDER, R. W. S., LANZEN, J., and MOORE, P. A. 1998. Boundary-layer effect on chemical signal movement near the antennae of the sphinx moth, *Manduca sexta*: Temporal filters for olfaction. *J. Comp. Physiol. A* 182:287–298.

SPARROW, E. M., HUSAR, R. B., and GOLDSTEIN, R. J. 1970. Observations and other characteristics of thermals. *J. Fluid Mech.* 41:793–800.

STEINBRECHT, R. A. 1970. Zur Morphometrie der Antenne des Seidenspinners, *Bombyx mori* (L.): Zahl und Verteilung der Riechsensillen (Insecta, Lepidoptera). *Z. Morphol. Tiere* 68:93–126.

STEINBRECHT, R. A. 1987. Functional morphology of pheromone-sensitive sensilla, pp. 353–384, *in* G. D. Prestwich and G. J. Blomquist (eds.). Pheromone Biochemistry. Academic Press, London.

STEINBRECHT, R. A. 1999. Olfactory receptors, pp. 155–176, *in* E. Eguchi and Y. Tominaga (eds.). Atlas of Arthropod Sensory Receptors. Springer-Verlag, Tokyo.

VICKERS, N. J. and BAKER, T. C. 1994. Reiterative responses to single str and s of odor promote sustained upwind flight and odor source location by moths. *Proc. Natl. Acad. Sci. USA* 91:5756–5760.

VICKERS, N. J., CHRISTENSEN, T. A., BAKER, T. C., and HILDEBRAND, J. G. 2001. Odour-plume dynamics influence the brain's olfactory code. *Nature* 410:466–470.

VOGEL, S. 1983. How much air passes through a silkmoth's antenna? *J. Insect Physiol.* 29:597–602.

VOGEL, S. 1994. Life in Moving Fluids: The Physical Biology of Flow. Princeton University Press, Princeton.

VOGEL, S. 2003. Comparative Biomechanics: Life's Physical World. Princeton University Press, Princeton.

WEAST, R. C., ASTLE, M. J., and BEYER, W. H. 1988. CRC Handbook of Chemistry and Physics. CRC Press, Boca Raton, FL.

WHITE, F. M. 1991. Viscous Fluid Flow. McGraw-Hill, Inc., New York.

WILLIS, M. A., DAVID, C. T., MURLIS, J., and CARDÉ, R. T. 1994. Effects of pheromone plume structure and visual stimuli on the pheromone-modulated upwind flight of male gypsy moths (*Lymantria dispar*) in a forest (Lepidoptera: Lymantriidae). *J. Insect Behav.* 7:385–409.

ZHANG, J. 2001. Investigation of the fluid mechanical properties of air flow around insects' antennae and implications for pheromone interception. PhD Dissertation. University of Kansas, Lawrence.